Multi-quasiparticle excitation: Extending shape coexistence in $A \sim 190$ neutron-deficient nuclei

Yue Shi,[1] F. R. Xu,[1,2,*] H. L. Liu,[1] and P. M. Walker[3]

[1]*School of Physics, and State Key Laboratory of Nuclear Physics and Technology, Peking University, Beijing 100871, China*

[2]*Center for Theoretical Nuclear Physics, National Laboratory for Heavy Ion Physics, Lanzhou 730000, China*

[3]*Department of Physics, University of Surrey, Guildford, Surrey GU2 7XH, United Kingdom*

(Received 9 July 2010; revised manuscript received 23 September 2010; published 21 October 2010)

Multi-quasiparticle high-K states in neutron-deficient mercury, lead, and polonium isotopes have been investigated systematically by means of configuration-constrained potential-energy-surface calculations. An abundance of high-K states is predicted with both prolate and oblate shapes, which extends the shape coexistence of the mass region. Well-deformed shapes provide good conditions for the formation of isomers, as exemplified in ^{188}Pb. Of particular interest is the prediction of low-lying 10^- states in polonium isotopes, which indicate long-lived isomers.

DOI: 10.1103/PhysRevC.82.044314 PACS number(s): 21.10.−k, 23.20.Lv, 27.70.+q, 27.80.+w

I. INTRODUCTION

The shape-coexistence phenomenon in the $A \sim 80$ and 190 mass regions has been a subject of considerable interest over a number of years [1–3]. Recent experimental progress in the identification of low-lying shape-coexisting 0^+ states in ^{186}Pb has led to renewed interest in this topic [4]. Indeed, the shape coexistence in lead nuclei around $N = 104$ may represent one of the most dramatic manifestations of this phenomenon. Owing to the presence of the $Z = 82$ shell closure, the ground states (g.s.) of neutron-deficient lead isotopes are dominated by sphericity, with two different shapes (oblate and prolate) coexisting at low excitation energies ($\lesssim$3 MeV). For even-even nuclei, one of the most important experimental fingerprints of shape coexistence is the observation of different low-lying 0^+ states with respective rotational bands. At least one low-lying 0^+ state with excitation energy below 1.0 MeV has, to date, been observed in all even-even lead isotopes with neutron numbers ranging from 100 to 112. Rotational bands based on both prolate [5–7] and oblate [8,9] shapes have been observed in ^{186,188}Pb.

From a shell-model point of view, the appearance of low-lying excited 0^+ states in lead isotopes stems from proton 2p-2h and 4p-4h (or 6p-6h) excitations across the $Z = 82$ shell closure. Potential-energy-surface (PES) calculations, however, show rather soft deformations for neutron-deficient lead and polonium isotopes, indicating considerable mixing between bands with different shapes (see, e.g., Refs. [10,11]). This has been confirmed experimentally by the observation of $E0$ components in $J \rightarrow J$ transitions at low spins between bands that arise from different shapes in ^{188}Pb [12], which is known to be a signature of shape mixing [13]. The mixing between different shapes is itself an interesting issue, although this may lead to considerable difficulty in isolating different shapes. One should notice that it is the shape mixing that complicates significantly the shape interpretations of the low-lying band structures in light polonium isotopes [3,14]. In practice, a two- or three-level-mixing analysis [15,16] or even a more sophisticated model [17,18] is needed to account for the shape mixing.

The shallow (soft) deformed subminima in the PES can be stabilized by collective rotation that can cause Coriolis mixing of high-j orbits which have strong deformation-driving effects. To increase the stability of soft deformation, another mechanism discussed in the present work is multi-quasiparticle excitation, which can cause shape polarization owing to unpaired nucleons. It is shown that the occupation of high-Ω orbits by unpaired nucleons can polarize the nuclei to be strongly deformed [19]. Well-deformed axial shapes, combined with low excitation energies, give good conditions for the formation of high-K isomers [20]. Owing to the possibility of increased stability, isomeric states in the unstable neutron-deficient nuclei would be advantageous for experimental measurements, with their decays providing useful structure information [12]. Indeed, significant progress has been made in the measurement of isomers in the most neutron-deficient lead isotopes [3]. In ^{188}Pb, for example, three spin isomers with different shapes have been identified and characterized by measuring rotational bands built upon them [12,21].

Another interesting feature in this mass region is the occurrence of oblate-deformed high-K isomers arising from the filling of strongly oblate-driving high-Ω orbits. Compared to prolate shape, it is rare for nuclei to have oblate deformation. The importance of oblate shapes is not only attributable to their rare occurrence, but also because the small number of oblate shapes may have a direct link to the detailed form of the mean-field potential [22,23]. The observation of a region of nuclei with stable oblate shapes would thus form an interesting testing ground for various mean-field models. Moreover, insight into the shell structure of nucleon orbits at oblate shape can be obtained from the excitation energies and configurations of isomers.

In this work we investigate the shape-coexistence phenomenon of two-quasiparticle isomeric states in the $A \sim 190$ mass region at both prolate and oblate deformations by means of configuration-constrained PES calculations. At oblate shapes, we give predictions of high-K states in

*frxu@pku.edu.cn

neutron-deficient lead and polonium isotopes. At prolate deformations, our main attention has been paid to systematic prediction of isomers in the $N = 102$ and 104 isotones. For this purpose, we extend our calculations to the lighter $N = 102$ and 104 isotones where more experimental information is available. Another goal of the present work is to study the shape polarization effect from multi-quasiparticle excitations.

II. THE MODEL

We have used the macroscopic-microscopic model with the standard liquid-drop energy [24] and microscopic shell and pairing corrections. Single-particle levels that are needed in the calculation of the microscopic energy are given by the nonaxial deformed Woods-Saxon (WS) potential with the set of universal parameters [25]. To avoid the possible collapse of pairings in multi-quasiparticle states, the approximate particle-number conservation by means of the Lipkin-Nogami (LN) pairing [26] has been employed with monopole pairing considered. The energy calculation of the macroscopic-microscopic model is standard as given, for example, in Ref. [27]. For a multi-quasiparticle state, however, the microscopic energy contains the contribution from the unpaired particles that occupy the single-particle orbits specified by the given configuration (see our previous work [28] for the detailed formula). Blocking effects from the unpaired particles are taken into account by removing the configuration orbits in the LN-pairing calculation.

In the macroscopic-microscopic model, the deformation of a state is obtained by minimizing the corresponding PES. The configuration-constrained PES calculation [28] for a multi-quasiparticle state requires the adiabatic blockings of the configuration orbits in the considered deformation space (β_2, γ, β_4); that is, the specific single-particle orbits are kept singly occupied while changing the deformation in the PES calculation. This has been achieved by calculating and identifying the average Nilsson quantum numbers of every orbit involved in the configuration [28]. The energy of a multi-quasipartcle state can be decomposed into the deformation energy and the configuration energy that corresponds to the quasiparticle excitations that undergo the pair breakings and excitations of the particles involved in the configuration. Owing to the polarization of the quasiparticle excitations, the deformation of a multi-quasipartcle state can be different from the one of the ground state. The shape polarization can be significant in a deformation-soft nucleus and result in a remarkably different deformation energy from that of the ground state. It has been shown that the self-consistent energy-deformation calculation by means of the configuration-constrained PES is very powerful to give the right deformation and energy of a multi-quasipartcle state [19,28]. In the present model, the excitation energy which can be compared with the experimental energy is obtained by the energy difference between the minima of the multi-quasiparticle and ground-state PESs. We discuss more about the calculations of excitation energies which are important for predictions or comparisons with experimental data.

The pairing strength, G, is an important factor that affects the energy calculation [28]. As done in previous works [19,28], the pairing strength (G) is determined first by the average gap method [29] and then adjusted to reproduce the experimental odd-even mass difference using a five-point formula in both experiment and theory. For nuclei in the valley of magic numbers, however, it has been pointed out that there are irregularities in the mass difference and thus the closed-shell nuclei are excluded in the determination of pairing strength [29]. Therefore, we take the standard G [29] for lead and polonium isotopes.

III. CALCULATIONS AND DISCUSSIONS

$K^\pi = 11^-, \pi\{9/2^-[505], 13/2^+[606]\}$, isomers have been observed systematically in even-even $^{188-196}$Pb and $^{194-210}$Po [3], with the configuration confirmed by g-factor measurements in ^{196}Pb [30] and ^{198,200}Po [31]. $K^\pi = 8^+$ isomers have also been found experimentally in $^{188-196}$Pb and $^{198-210}$Po [3]. The configuration of the 8^+ isomers has been assigned to be $\pi\{9/2^-[505], 7/2^-[514]\}$ confirmed also by g-factor measurements in ^{198,200}Po [31]. The proton Nilsson diagram shows that many oblate-driving high-Ω orbits appear around the Fermi surface of $Z \approx 82$ at the oblate side of $\beta_2 \approx 0.2$, which has been seen in the neighboring odd-Z nuclei as isomeric states. It may be expected that high-K states with even lower energies and larger deformations could exist in polonium isotopes because the proton Fermi level for $Z = 84$ is located among these high-Ω orbits.

We have performed systematic calculations for lead and polonium isotopes with $N = 104$–116. Table I lists the detailed results for the oblate isomers in lead isotopes, including available experimental energies. As examples, Fig. 1 displays configuration-constrained PESs for the predicted prolate 6^- and oblate 11^- states (the prolate states are discussed later). For systematic comparisons, we plot energies and deformations that can be obtained experimentally in Fig. 2 for the oblate states. It can be seen that the overall agreement between calculations and data for the observed 11^- and 8^+ isomers in lead isotopes is reasonably good. The calculations reproduce the experimental behavior of energies changing with neutron number but overestimate the energies in heavier lead isotopes. The discrepancy between measurements and calculations grows from about 100 keV in ^{188}Pb to 500 keV in ^{196}Pb. The oblate $|\beta_2|$ values for the 11^- and 8^+ isomers in lead isotopes decrease smoothly from 0.19 in ^{186}Pb to 0.15 in ^{198}Pb. For comparison, three available experimental β_2 values extracted from the measured spectroscopic quadrupole moments in $^{192-196}$Pb [32,33] are given. We see that the calculations reproduce well the experimental deformations in ^{194,196}Pb, but give a smaller deformation in ^{192}Pb. The energies and deformations obtained in the present work are consistent with previous Nilsson-Strutinsky [10] and Skyrme-HFB [33,34] calculations that were limited to axially symmetric shapes.

Compared with the situation in the lead isotopes, the shape-coexistence phenomenon is less established in the polonium isotopes. For the lead isotopes investigated, the ground states are always spherical and the 0_2^+ states have oblate shapes, as shown in Fig. 2. This is consistent with results given by the Skyrme-HFB calculations [34]. For the polonium isotopes, the PESs are more complicated. Figure 3 displays potential

TABLE I. Calculated excitation energies, deformations, and quadrupole moments of the oblate two-quasiparticle isomeric states in lead isotopes. The experimental data can be found in Refs. [3,32,33] and references therein. Note that a negative β_2 value corresponds to a $\gamma = 60^\circ$ oblate shape.

Nuclei	K^π	Configurations	β_2	β_4	$Q_{20}^{\rm cal}$ (eb)	$Q_{20}^{\rm exp}$ (eb)	$E_{\rm ex}^{\rm cal}$ (keV)	$E_{\rm ex}^{\rm exp}$ (keV)
^{186}Pb	0^+	g.s.	0.01	0.00	0.00		0	0
	11^-	$\pi\{13/2^+[606], 9/2^-[505]\}$	−0.19	0.01	−5.34		3021	
	10^-	$\pi\{13/2^+[606], 7/2^-[514]\}$	−0.21	0.01	−6.54		3482	
	8^+	$\pi\{9/2^-[505], 7/2^-[514]\}$	−0.18	0.01	−5.71		2623	
^{188}Pb	0^+	g.s.	0.01	0.00	0.00		0	0
	8^+	$\nu\{9/2^+[624], 7/2^+[633]\}$	−0.18	0.00	−5.80		2638	
	11^-	$\pi\{13/2^+[606], 9/2^-[505]\}$	−0.19	0.01	−5.42		2810	2713
	10^-	$\pi\{13/2^+[606], 7/2^-[514]\}$	−0.22	0.01	−6.77		3268	
	10^-	$\pi\{11/2^+[615], 9/2^-[505]\}$	−0.18	−0.01	−5.75		3898	
	8^+	$\pi\{9/2^-[505], 7/2^-[514]\}$	−0.18	0.01	−5.72		2428	2216
^{190}Pb	0^+	g.s.	0.01	0.00	0.00		0	0
	8^+	$\nu\{9/2^+[624], 7/2^+[633]\}$	−0.17	0.00	−5.71		2764	
	11^-	$\pi\{13/2^+[606], 9/2^-[505]\}$	−0.19	0.00	−5.46		2809	2658
	10^-	$\pi\{13/2^+[606], 7/2^-[514]\}$	−0.22	0.01	−6.70		3300	
	10^-	$\pi\{11/2^+[615], 9/2^-[505]\}$	−0.18	−0.01	−5.72		3840	
	8^+	$\pi\{9/2^-[505], 7/2^-[514]\}$	−0.18	0.01	−5.76		2431	2252
^{192}Pb	0^+	g.s.	0.01	0.00	0.00		0	0
	11^-	$\pi\{13/2^+[606], 9/2^-[505]\}$	−0.18	0.00	−5.37	−3.5(4)	3009	2743.5
	10^-	$\pi\{13/2^+[606], 7/2^-[514]\}$	−0.21	0.00	−6.49		3606	
	10^-	$\pi\{11/2^+[615], 9/2^-[505]\}$	−0.17	−0.02	−5.58		3928	
	8^+	$\pi\{9/2^-[505], 7/2^-[514]\}$	−0.17	0.00	−5.22		2609	2304
^{194}Pb	0^+	g.s.	0.01	0.00	0.00		0	0
	11^-	$\pi\{13/2^+[606], 9/2^-[505]\}$	−0.17	−0.01	−5.15	−4.3(5)	3284	2933
	8^+	$\pi\{9/2^-[505], 7/2^-[514]\}$	−0.16	0.00	−4.89		2867	2437.4
^{196}Pb	0^+	g.s.	0.01	0.00	0.00		0	0
	11^-	$\pi\{13/2^+[606], 9/2^-[505]\}$	−0.16	−0.01	−4.74	−4.1(8)	3598	3192.2
	8^+	$\pi\{9/2^-[505], 7/2^-[514]\}$	−0.15	−0.01	−4.70		3153	2621.9
^{198}Pb	0^+	g.s.	0.01	0.00	0.00		0	0
	11^-	$\pi\{13/2^+[606], 9/2^-[505]\}$	−0.15	−0.02	−4.36		3931	
	8^+	$\pi\{9/2^-[505], 7/2^-[514]\}$	−0.14	−0.01	−3.88		3447	

energy curves as the function of β_2 deformation. At each β_2 point, the energy has been minimized with respect to the β_4 parameter. We see that the seniority-zero 0^+ energy curves are very soft against deformations, which is consistent with the experimental observation of the vibrational property of low-lying states in ^{194,196}Po [35]. In Ref. [3], it was commented that the low-lying states would have shape mixing with 2p and 4p-2h configurations. Our calculations show oblate minima at $\beta_2 \approx -0.2$ in $^{188-196}$Po and prolate minima at $\beta_2 \approx 0.25$ in ^{188,190}Po. Weak and soft deformations with $|\beta_2| < 0.1$ exist in the polonium isotopes, which would indicate nearly spherical shapes. The calculated energy curves are in general similar to those obtained by the Skyrme-HFB model [34], giving similar conclusions about shape coexistences in the isotopes. These calculations are also consistent with the previous PES calculations [16].

Experimentally, the lowest 2^+ and 4^+ states in heavier polonium isotopes with $N \leqslant 116$ have approximately constant excitation energies [3]. These nuclei can be considered as nearly spherical anharmonic vibrators [3]. For even-even polonium isotopes lighter than ^{198}Po, the energies of the yrast band members undergo a progressive decrease with decreasing neutron number (e.g., see Fig. 24 of Ref. [3]). This has been taken as evidence that the systems start to evolve toward more collectivity through mixing [36], which is consistent with our calculations in which oblate minima arise in the isotopes lighter than ^{198}Po. Recent experiments have confirmed the mixing scenario in ^{194}Po [14]. For ^{190}Po, low-lying band structure with prolate shape has been observed [37], which is also consistent with our calculation.

Now we investigate multi-quasiparticle states in the polonium isotopes. We have made detailed theoretical search for possible low-lying two-quasiparticle high-K states, given in Table II with calculated excitation energies and deformations. The two-quasiproton $\pi\{13/2^+[606], 9/2^-[505]\}$ $K^\pi = 11^-$ states are of particular interest, which have been observed experimentally to be isomers in $^{194-200}$Po and investigated extensively in both experiments [3] and theories [10,34]. The experimental excitation energies of the 11^- isomers are about 2.5 MeV. A recent experiment observed a 580(100)-ns isomer

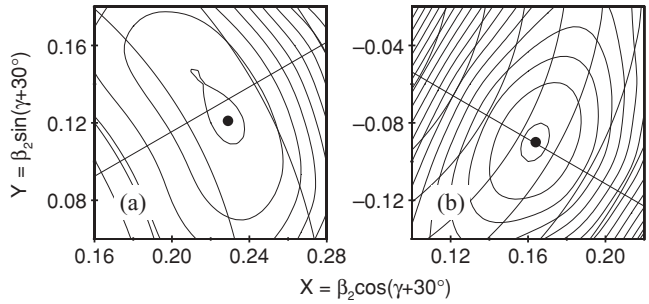

FIG. 1. Configuration-constrained PESs for the *prolate* $K^\pi = 6^-$ ($\nu\{7/2[633], 5/2[512]\}$) state (a) and the *oblate* $K^\pi = 11^-$ ($\pi\{13/2[606], 9/2[505]\}$) state (b) in ^{186}Pb. The calculated deformations and excitation energies can be found in Tables I and III. The energy difference between neighboring contours is 100 keV. The intrinsic PESs are reflection-symmetric about $\gamma = 0°$; that is, the shape with $\gamma = -60°$ is the same as the one with $\gamma = 60°$ for noncollective excitations.

deexciting via a 154-keV transition to the 10^+ member of the collective band in ^{192}Po [38]. The $E1$ multipolarity of the 154-keV transition is indicative of an 11^- isomer at an excitation energy of 2295 keV. The calculated configuration-constrained PESs are displayed in Fig. 3. We see that the 11^- isomeric states have soft oblate shapes. In the ^{194}Po case, it seems that there are two minima at $\beta_2 \approx -0.2$ and $\beta_2 \approx -0.1$, respectively, with a low barrier between them. From ^{194}Po to ^{196}Po, the lowest minimum moves from $\beta_2 \approx -0.2$ to $\beta_2 \approx -0.1$, respectively, which has also been shown in Fig. 2.

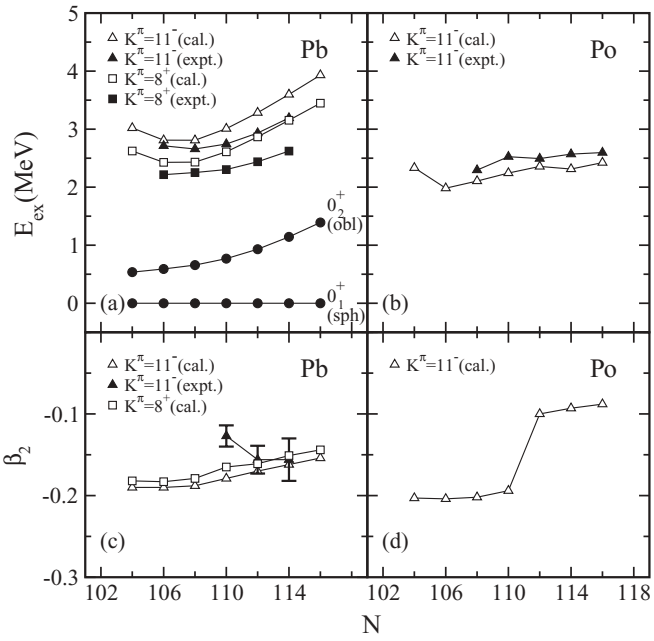

FIG. 2. Excitation energies [panels (a) and (b)] and the corresponding β_2 deformations [panels (c) and (d)] for $\pi\{13/2^+[606], 9/2^-[505]\}$ ($K^\pi = 11^-$) and $\pi\{7/2^-[514], 9/2^-[505]\}$ ($K^\pi = 8^+$) oblate states in lead and polonium isotopes. The experimental data are from Refs. [3,32,33]. In (a), the black dots give the experimental energies of the 0_1^+ (spherical) and 0_2^+ (oblate) states.

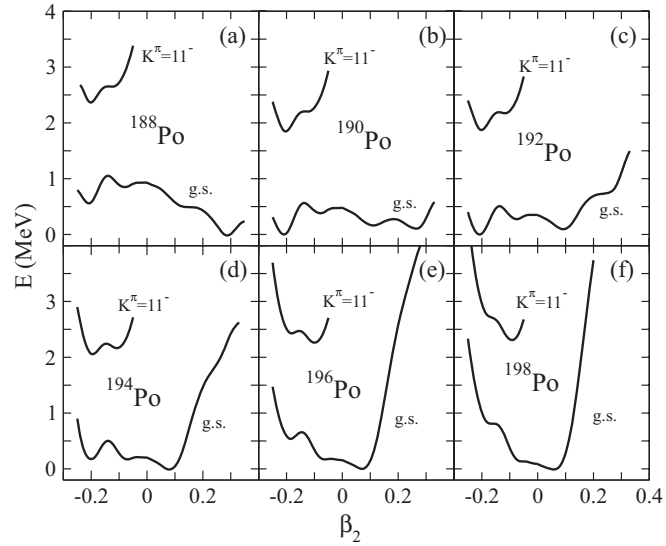

FIG. 3. Potential energy curves against β_2 deformation for seniority-zero $K^\pi = 0^+$ (i.e., no quasiparticle excitation) and two-quasiproton $\pi\{13/2^+[606], 9/2^-[505]\}$ $K^\pi = 11^-$ states in neutron-deficient even-even polonium isotopes. The lowest minimum in the seniority-zero curve (marked by g.s.) gives the ground state.

However, this would not imply a real abrupt change of the deformation. It would be more reasonable to conclude that the 11^- states in ^{194,196}Po have soft oblate deformations with β_2 between -0.2 and -0.1.

It has been explained that the excitation energy is obtained in the present model by the energy difference between the minima of the multi-quasiparticle and ground-state PESs. For deformation-soft states, however, the configuration mixing (or called deformation mixing) would be remarkable [34]. The authors of Ref. [34] have performed configuration-mixing calculations within the generator coordinate method (GCM) for the 0^+ states of the shape-soft polonium isotopes, giving that the mixing can make eigenenergies deviate from the PES minima. However, we notice that the energy difference between the 0_2^+ and 0_1^+ eigenstates obtained in the GCM calculations is in general similar to the energy difference between the second and the first minima given by the PES [34]. In the present model, we may expect that deformation-mixing effects on energies are canceled at least partly owing to the similar softnesses of the seniority-zero 0^+ and two-quasiparticle 11^- PESs near the minima. Therefore, the excitation energy obtained by the PES minima should be an acceptable approximation for a multi-quasiparticle state. This has been well evidenced in our calculations including the previous works [19,28], compared with experimental data. The lead isotopes have well-defined spherical ground states and oblate multi-quasiparticle states. In Ref. [34] the PES minima have been taken in the determinations of energies and deformations for the lead isotopes, which has also been justified by configuration-mixing calculations [39–42], indicating that deformation-mixing effect is less significant in these isotopes. Therefore, the calculations of excitation energies by PES minima should be more accurate for the multi-quasiparticle states of the lead isotopes.

TABLE II. Similar to Table I, but for polonium isotopes.

Nuclei	K^π	Configurations	β_2	β_4	$Q_{20}^{\rm cal}$ (eb)	$E_{\rm ex}^{\rm cal}$ (keV)	$E_{\rm ex}^{\rm exp}$ (keV)
^{188}Po	0^+	g.s.	0.29	0.01	10.86	0	0
	11^-	$\pi\{13/2^+[606], 9/2^-[505]\}$	−0.20	0.01	−6.01	2422	
	10^-	$\pi\{13/2^+[606], 7/2^-[514]\}$	−0.21	0.02	−6.92	1697	
	10^-	$\pi\{11/2^+[615], 9/2^-[505]\}$	−0.20	0.01	−6.01	3307	
	9^-	$\pi\{11/2^+[615], 7/2^-[514]\}$	−0.21	0.01	−6.54	2843	
^{190}Po	0^+	g.s.	−0.21	0.01	−6.78	0	0
	8^+	$\nu\{9/2^+[624], 7/2^+[633]\}$	−0.21	−0.01	−6.87	1611	
	6^-	$\nu\{7/2^+[633], 5/2^-[503]\}$	−0.20	0.00	−6.46	2269	
	11^-	$\pi\{13/2^+[606], 9/2^-[505]\}$	−0.20	0.01	−6.49	1960	
	10^-	$\pi\{13/2^+[606], 7/2^-[514]\}$	−0.21	0.02	−6.94	1212	
	10^-	$\pi\{11/2^+[615], 9/2^-[505]\}$	−0.21	0.00	−6.10	2830	
	9^-	$\pi\{11/2^+[615], 7/2^-[514]\}$	−0.21	0.01	−6.56	2352	
^{192}Po	0^+	g.s.	−0.20	0.00	−6.70	0	0
	8^+	$\nu\{9/2^+[624], 7/2^+[633]\}$	−0.20	−0.01	−6.55	1839	
	6^-	$\nu\{7/2^+[633], 5/2^-[503]\}$	−0.21	0.00	−6.71	1710	
	11^-	$\pi\{13/2^+[606], 9/2^-[505]\}$	−0.20	0.01	−6.49	1923	
	10^-	$\pi\{13/2^+[606], 7/2^-[514]\}$	−0.21	0.01	−7.01	1168	
	10^-	$\pi\{11/2^+[615], 9/2^-[505]\}$	−0.20	0.00	−6.00	2771	
	9^-	$\pi\{11/2^+[615], 7/2^-[514]\}$	−0.21	0.01	−6.49	2300	
^{194}Po	0^+	g.s.	0.07	0.01	2.90	0	0
	8^+	$\nu\{9/2^+[624], 7/2^+[633]\}$	−0.08	−0.01	−2.93	2087	
	6^+	$\nu\{7/2^+[633], 5/2^+[642]\}$	−0.20	0.00	−6.43	1668	
	6^-	$\nu\{7/2^+[633], 5/2^-[503]\}$	−0.20	0.00	−6.43	1721	
	11^-	$\pi\{13/2^+[606], 9/2^-[505]\}$	−0.19	0.00	−5.93	2096	2525.2
	10^-	$\pi\{13/2^+[606], 7/2^-[514]\}$	−0.21	0.01	−6.69	1381	
	10^-	$\pi\{11/2^+[615], 9/2^-[505]\}$	−0.19	−0.01	−6.42	2910	
	9^-	$\pi\{11/2^+[615], 7/2^-[514]\}$	−0.20	0.01	−6.14	2489	
^{196}Po	0^+	g.s.	0.06	0.00	2.51	0	0
	8^+	$\nu\{9/2^+[624], 7/2^+[633]\}$	−0.08	−0.01	−2.78	2190	
	11^-	$\pi\{13/2^+[606], 9/2^-[505]\}$	−0.10	0.02	−3.66	2287	2493
	10^-	$\pi\{13/2^+[606], 7/2^-[514]\}$	−0.19	0.01	−6.03	1825	
	10^-	$\pi\{11/2^+[615], 9/2^-[505]\}$	−0.18	−0.02	−5.94	3206	
	9^-	$\pi\{11/2^+[615], 7/2^-[514]\}$	−0.19	0.00	−6.25	2874	
^{198}Po	0^+	g.s.	−0.06	0.00	−2.21	0	0
	8^+	$\nu\{9/2^+[624], 7/2^+[633]\}$	−0.07	−0.01	−2.94	2289	
	11^-	$\pi\{13/2^+[606], 9/2^-[505]\}$	−0.10	0.01	−3.40	2302	2565.9
	10^-	$\pi\{13/2^+[606], 7/2^-[514]\}$	−0.18	0.00	−5.89	2199	
	9^-	$\pi\{11/2^+[615], 7/2^-[514]\}$	−0.18	0.01	−6.12	3169	
^{200}Po	0^+	g.s.	0.05	0.00	1.92	0	0
	11^-	$\pi\{13/2^+[606], 9/2^-[505]\}$	−0.09	0.01	−3.30	2423	2596
	10^-	$\pi\{13/2^+[606], 7/2^-[514]\}$	−0.17	0.00	−5.84	2629	
	9^-	$\pi\{11/2^+[615], 7/2^-[514]\}$	−0.17	−0.01	−5.70	3534	

Figure 2 shows comparisons with experimental energies for the $K^\pi = 11^-$ isomeric states. We see that experimental energies are reproduced reasonably. In the lead isotopes, the 11^- isomers (and also the 8^+ isomers) have a trend of increasing energy with neutron number, in a similar way to the oblate 0_2^+ states (see Fig. 2). This is easily understood because the isomers are built on the oblate minima. Experiments have confirmed that the oblate 0_2^+ states are always higher than the spherical 0_1^+ states and the energies increase monotonically with increasing neutron number (shown in Fig. 2). In the polonium isotopes, the deformation-soft 11^- states are also constructed on oblate minima, while the situation for the 0^+ minima is complicated with the possible coexistence of oblate, prolate, and nearly spherical shapes, as discussed earlier. The systematic underestimation of ≈200–400 keV in the polonium isotopes may indicate the effect from the deformation mixing. However, as another possibility which has been observed in the previous works [19,28], systematic discrepancies between calculated and experimental energies would be related to pairing strengths taken in the

TABLE III. Similar to Table I, but for the two-quasineutron 7^-, 6^-, and 6^+ states in $N = 102$ and $N = 104$ isotones, with the configurations of $\nu\{7/2^+[633], 7/2^-[514]\}$, $\nu\{7/2^+[633], 5/2^-[512]\}$, and $\nu\{7/2^-[514], 5/2^-[512]\}$, respectively. $\gamma \approx 0^\circ$ for all the states except the ^{184}Pb 6^+ state that has $\gamma \approx 15^\circ$. The experimental energies can be found in Refs. [46,48,54] and references therein.

Nuclei	K^π	β_2	β_4	$Q_{20}^{\rm cal}$ (eb)	$E_{\rm ex}^{\rm cal}$ (keV)	$E_{\rm ex}^{\rm exp}$ (keV)
$^{176}_{74}W_{102}$	7^-	0.30	−0.02	9.29	1786	
	6^-	0.27	−0.01	8.15	1531	
	6^+	0.25	−0.02	7.50	1795	
$^{178}_{74}W_{104}$	7^-	0.25	−0.03	7.49	1696	1738
	6^-	0.25	−0.02	7.52	1860	
	6^+	0.26	−0.03	7.78	1594	1665
$^{178}_{76}Os_{102}$	7^-	0.22	−0.02	6.43	1870	
	6^-	0.24	−0.01	7.33	1766	
	6^+	0.22	−0.02	6.43	1873	
$^{180}_{76}Os_{104}$	7^-	0.22	−0.03	6.56	1816	1930
	6^-	0.22	−0.02	6.46	1954	
	6^+	0.23	−0.03	6.90	1832	1878
$^{180}_{78}Pt_{102}$	7^-	0.23	−0.01	7.16	1981	
	6^-	0.25	0.00	8.07	1827	
	6^+	0.23	−0.01	7.16	1981	
$^{182}_{78}Pt_{104}$	7^-	0.23	−0.02	7.09	1989	1955
	6^-	0.23	−0.01	7.25	2053	
	6^+	0.25	−0.03	8.00	2020	
$^{182}_{80}Hg_{102}$	7^-	0.25	0.00	8.39	2075	
	6^-	0.26	0.00	8.90	1853	
	6^+	0.24	0.00	7.93	2094	
$^{184}_{80}Hg_{104}$	7^-	0.24	−0.01	7.99	2285	
	6^-	0.25	−0.01	8.39	2452	
	6^+	0.26	−0.01	8.83	2094	
$^{184}_{82}Pb_{102}$	7^-	0.27	0.01	10.15	2296	
	6^-	0.27	0.01	10.15	1978	
	6^+	0.26	0.01	9.72	2300	
$^{186}_{82}Pb_{104}$	7^-	0.26	−0.01	9.50	2659	
	6^-	0.26	−0.01	9.50	2846	
	6^+	0.27	−0.01	10.04	2310	

present model. A slight increase of the pairing strength can significantly increase the excitation energies of multi-quasiparticle states [19,28]. The systematic overestimation for the energies of the 11^- and 8^- isomers in the lead isotopes can be explained by a slight decrease of the proton pairing strength.

In addition to the 11^- and 8^+ isomers observed systematically, we see in Tables I and II that many other two-quasiparticle high-K states are predicted to exist in the neutron-deficient lead and polonium isotopes with excitation energies lower than 3.5 MeV. Of particular interest is that in the polonium isotopes the two-proton 10^- states with the configuration of $\pi\{13/2^+[606], 7/2^-[514]\}$ are predicted to have lower energies than other two-quasiparticle states, including the observed 11^- isomers. The low excitation energies indicate the possibility of long-lived 10^- states, which would be interesting to observe in future experiments. The high-K states provide good settings for the study of oblate deformations and the shape-coexistence phenomenon in the neutron-deficient lead and polonium isotopes.

For a multi-quasiparticle state, the quadrupole moment and g factor are other important observables that provide direct information on the deformation and configuration. In the present model, the intrinsic quadrupole moment is calculated by $Q_{20} = \sum q_{k_j} + \sum_{k\neq k_j} 2V_k^2 q_k$, where q_k is the single-particle quadrupole moment of the kth orbit given in the WS model. The first term gives the contribution from the unpaired particles that stay on the k_jth orbit, and the second term is from all the paired particles that occupy the WS orbits with probabilities V_k^2 in the LN pairing model. Blocking effects are taken into account by restricting $k \neq k_j$ in the sum. The quadrupole moment thus calculated is configuration dependent. In Tables I, II, and III, we predict quadrupole moments for multi-quasiparticle and ground states. The present model is not suitable, in its present form, for the calculation of g factors. This will be the subject of future work.

Experimental information concerning prolate high-K isomers in mercury and lead isotopes is relatively scarce. The only known cases are the two-quasineutron $K^\pi = 8^-$ ($\nu\{7/2^-[514], 9/2^+[624]\}$) states observed in ^{186}Hg [43] and ^{188}Pb [12] with $N = 106$. In the $N = 104$ isotones, the dominance of the 8^- intrinsic state is taken over by the favored $K^\pi = 6^+$ ($\nu\{7/2^-[514], 5/2^-[512]\}$) and 7^- ($\nu\{7/2^+[633], 7/2^-[514]\}$) states. The 6^+ isomers have been observed from ^{172}Er to ^{180}Os with half-lives ranging from several μs to a few ns [44,45]. The 7^- isomers have been seen in ^{178}W [46], ^{180}Os [47], and ^{182}Pt [48]. For $N = 102$ isotones, a $K^\pi = 6^-$ state with the configuration of $\nu\{7/2^+[633], 5/2^-[512]\}$ was observed in ^{172}Yb [49], ^{174}Hf [50], and probably ^{170}Er [51]. These three configurations have not been observed in the heavier isotones of $N = 104$ and 102, although similar band structure that might be associated with a K isomer has been observed in ^{184}Hg [52]. We note that the $K^\pi = 6^-$ $\nu\{7/2^+[633], 5/2^-[512]\}$ configuration has an unfavored residual spin-spin interaction ($\approx$+300 keV) while the residual interaction is favored for the 6^+, 7^-, and 8^- configurations (≈ -100 keV) [53]. This would be a reason why the 6^- state is more difficult to observe compared with the neighboring $6^+, 7^-$, and 8^- states. The residual interactions are not included in the present calculations. In Ref. [19], the structures of the two-neutron 8^- ($\nu\{9/2^+[624], 7/2^-[514]\}$) isomers which have been observed systematically in the $N = 106$ isotones in this mass region were calculated, showing remarkable shape changes with proton number approaching the $Z = 82$. The quasiparticle excitations provide useful information about the shell structure of nucleon orbits. The calculations of high-K states, particularly the predictions of energies, can provide important guidance for future experimental investigations.

We therefore made a thorough search for a variety of possible multi-quasiparticle states along the $N = 104$ and 102 isotonic chains with $Z = 74$–82. Similar PES calculations for the 6^+ states have been reported in some $N = 104$ isotones [45]. The detailed calculations of energies and deformations are listed in Table III. For clear comparisons of energies and deformations, see also Fig. 4. Good agreements between experiments and calculations are obtained for the known 6^+ and 7^- states in the $N = 104$ isotones. Note that the observed 7^- 1.93-MeV state in ^{180}Os is expected to mix with the 7^- 1.86-MeV member of a side band [47]. The unperturbed levels should then lie closer. As an interesting example, the nucleus ^{186}Pb is calculated to have a spherical ground state and several prolate and oblate high-K states (see Fig. 1).

While almost all the ground states of the studied lead and polonium isotopes have relatively small deformations except for the polonium isotopes lighter than ^{194}Po, nearly all the calculated high-K states have well-deformed axial shapes (see Tables I and II), indicating significant shape polarizations from the pair-broken nucleons. Further, we found that the orbital blockings can stabilize the minimum of the configuration-constrained PES for these nuclei. The effect on the stability of states has also been seen in the superheavy nuclei where unpaired nucleons lead to higher and wider fission barriers for high-K states as compared to the respective ground states [55]. Compared with the ground states that have soft deformations, these relatively rigid high-K states are less susceptible to shape mixing, thus providing good opportunities for the study of shape coexistence in this mass region. Owing to the fact that the neutron-deficient polonium isotopes are close to the proton drip line and owing to the predominant fission channel, spectroscopic studies of these nuclei become increasingly difficult. The present calculations suggest that it may be possible to investigate these nuclei via the measurements of the high-K isomers. Experimentally, the shape-polarization effect that leads to larger deformation and more rigid shapes has been seen in odd-mass polonium isotopes in α-decay studies. In ^{191}Po, for example, two α-decaying isomers were observed to have remarkably different half-lives, which has been interpreted to be attributable to the large shape polarization from the odd nucleon. The authors of Ref. [56] noticed also that the longer-lived isomeric state is purer than the even-even neighbors. The observed low-spin band structures based on high-K orbits in odd-mass polonium isotopes have also shown more pronounced collectivity than in the neighboring even-even isotopes [57].

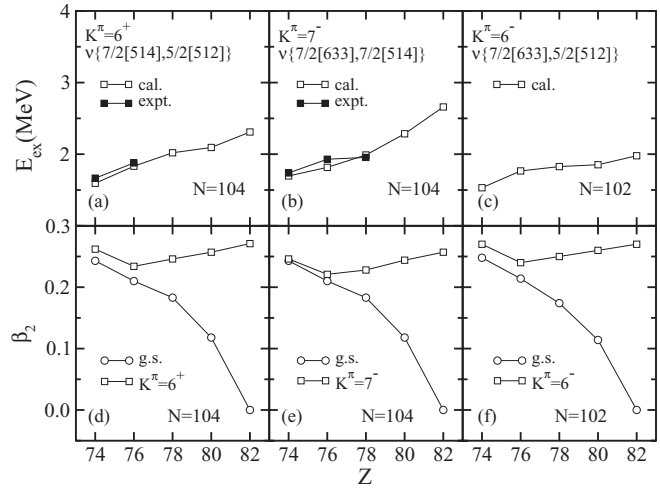

FIG. 4. Similar to Fig. 2, but for prolate high-K states in $N = 104$ and 102 isotones.

IV. SUMMARY

Configuration-constrained PES calculations have been performed to investigate the shape-coexistence phenomenon associated with high-K states in neutron-deficient mercury, lead, and polonium isotopes. A large number of oblate-shape high-K states are predicted to occur at low excitation energies in neutron-deficient lead and polonium isotopes. At prolate deformations, attention has been paid to the systematic prediction of high-K states along the $N = 102$ and 104 isotonic chains. Three high-K states, namely, $K^\pi = 7^-$, 6^-, and 6^+ with $\nu\{7/2^+[633], 7/2^-[514]\}$, $\nu\{7/2^+[633], 5/2^-[512]\}$, and $\nu\{7/2^-[514], 5/2^-[512]\}$ configurations, respectively, have been found. Good agreements between calculations and available data have been obtained. The high-K states open up new possibilities for the study of the shape-coexistence phenomenon in this mass region. Low excitation energies and large K-values, as well as rigid axially deformed shapes as

compared to their ground states, provide favorable conditions for the formation of isomers. The nucleus, ^{186}Pb, is calculated to have high-K isomers with distinct shapes (*oblate* and *prolate*) that coexist at similar excitation energies. It is remarkable that the oblate 10^- states with the two-proton configuration $\pi\{13/2^+[606], 7/2^-[514]\}$ are predicted to have significantly lower energies than other two-quasiparticle high-K states in the polonium isotopes. This would indicate long-lived isomers existing in the neutron-deficient polonium isotopes, and a corresponding experimental search is needed.

ACKNOWLEDGMENTS

This work has been supported by the Natural Science Foundation of China under Grants No. 10735010 and No. 10975006, the Chinese Major State Basic Research Development Program under Grant No. 2007CB815000, the UK STFC, and AWE plc.

[1] J. L. Wood, K. Heyde, W. Nazarewicz, M. Huyse, and P. Van Duppen, Phys. Rep. **215**, 101 (1992).
[2] K. Heyde, P. Van Isacker, M. Waroquier, J. L. Wood, and R. A. Meyer, Phys. Rep. **102**, 291 (1983).
[3] R. Julin, K. Helariutta, and M. Muikku, J. Phys. G **27**, R109 (2001).
[4] A. N. Andreyev *et al.*, Nature (London) **405**, 430 (2000).
[5] J. Heese, K. H. Maier, H. Grawe, J. Grebosz, H. Kluge, W. Meczynski, M. Schramm, R. Schubert, K. Spohr, and J. Styczen, Phys. Lett. B **302**, 390 (1993).
[6] A. M. Baxter *et al.*, Phys. Rev. C **48**, 2140(R) (1993).
[7] W. Reviol, C. J. Chiara, O. Pechenaya, D. G. Sarantites, P. Fallon, and A. O. Macchiavelli, Phys. Rev. C **68**, 054317 (2003).
[8] J. Pakarinen *et al.*, Phys. Rev. C **75**, 014302 (2007).
[9] G. D. Dracoulis, G. J. Lane, A. P. Byrne, T. Kibédi, A. M. Baxter, A. O. Macchiavelli, P. Fallon, and R. M. Clark, Phys. Rev. C **69**, 054318 (2004).
[10] R. Bengtsson and W. Nazarewicz, Z. Phys. A **334**, 269 (1989).
[11] F. R. May, V. V. Pashkevich, and S. Frauendorf, Phys. Lett. B **68**, 113 (1977).
[12] G. D. Dracoulis, G. J. Lane, A. P. Byrne, A. M. Baxter, T. Kibédi, A. O. Macchiavelli, P. Fallon, and R. M. Clark, Phys. Rev. C **67**, 051301(R) (2003).
[13] J. L. Wood, E. F. Zganjar, C. De Coster, and K. Heyde, Nucl. Phys. A **651**, 323 (1999).
[14] T. Grahn *et al.*, Phys. Rev. Lett. **97**, 062501 (2006).
[15] G. D. Dracoulis, Phys. Rev. C **49**, 3324 (1994).
[16] A. M. Oros, K. Heyde, C. De Coster, B. Decroix, R. Wyss, B. R. Barrett, and P. Navratil, Nucl. Phys. A **645**, 107 (1999).
[17] M. Bender, P. Bonche, T. Duguet, and P.-H. Heenen, Phys. Rev. C **69**, 064303 (2004).
[18] V. Hellemans, S. De Baerdemacker, and K. Heyde, Phys. Rev. C **77**, 064324 (2008).
[19] F. R. Xu, P. M. Walker, and R. Wyss, Phys. Rev. C **59**, 731 (1999).
[20] P. M. Walker and G. D. Dracoulis, Nature (London) **399**, 35 (1999).
[21] G. D. Dracoulis, A. P. Byrne, A. M. Baxter, P. M. Davidson, T. Kibédi, T. R. McGoram, R. A. Bark, and S. M. Mullins, Phys. Rev. C **60**, 014303 (1999).
[22] N. Tajima and N. Suzuki, Phys. Rev. C **64**, 037301 (2001).
[23] I. Hamamoto and B. R. Mottelson, Phys. Rev. C **79**, 034317 (2009).
[24] W. D. Myers and W. J. Swiatecki, Nucl. Phys. **81**, 1 (1966).
[25] W. Nazarewicz, J. Dudek, R. Bengtsson, T. Bengtsson, and I. Ragnarsson, Nucl. Phys. A **435**, 397 (1985).
[26] W. Satuła, R. Wyss, and P. Magierski, Nucl. Phys. A **578**, 45 (1994).
[27] P. Möller, J. R. Nix, W. D. Myers, and W. J. Swiatecki, At. Data Nucl. Data Tables **59**, 185 (1995).
[28] F. R. Xu, P. M. Walker, J. A. Sheikh, and R. Wyss, Phys. Lett. B **435**, 257 (1998).
[29] P. Möller and J. R. Nix, Nucl. Phys. A **536**, 20 (1992).
[30] J. Penninga, W. H. A. Hesselink, A. Balanda, A. Stolk, H. Verheul, J. van Klinken, H. J. Riezebos, and M. J. A. de Vorgt, Nucl. Phys. A **471**, 535 (1987).
[31] A. Maj, H. Grawe, H. Kluge, A. Kuhnert, K. H. Maier, J. Recht, N. Roy, H. Hübel, and M. Guttormsen, Nucl. Phys. A **509**, 413 (1990).
[32] K. Vyvey *et al.*, Phys. Rev. Lett. **88**, 102502 (2002).
[33] M. Ionescu-Bujor *et al.*, Phys. Lett. B **650**, 141 (2007).
[34] N. A. Smirnova, P.-H. Heenen, and G. Neyens, Phys. Lett. B **569**, 151 (2003).
[35] L. A. Bernstein *et al.*, Phys. Rev. C **52**, 621 (1995).
[36] D. Alber *et al.*, Z. Phys. A **339**, 225 (1991).
[37] K. Van de Vel *et al.*, Eur. Phys. J. A **17**, 167 (2003).
[38] K. Van de Vel *et al.*, Phys. Rev. C **68**, 054311 (2003).
[39] N. Tajima, H. Flocard, P. Bonche, J. Dobaczewski, and P.-H. Heenen, Nucl. Phys. A **551**, 409 (1993).
[40] R. R. Chasman, J. L. Egido, and L. M. Robledo, Phys. Lett. B **513**, 325 (2001).
[41] P.-H. Heenen, A. Valor, M. Bender, P. Bonche, and H. Flocard, Eur. Phys. J. A **11**, 393 (2001).
[42] T. Duguet, M. Bender, P. Bonche, and P.-H. Heenen, Phys. Lett. B **559**, 201 (2003).
[43] M. G. Porguet, G. Bastin, C. Bourgeois, A. Korichi, N. Perrin, H. Sergolle, and F. A. Beck, J. Phys. G **18**, L29 (1992).
[44] G. D. Dracoulis *et al.*, Phys. Lett. B **635**, 200 (2006).
[45] G. D. Dracoulis *et al.*, Phys. Rev. C **79**, 061303(R) (2009).
[46] C. S. Purry *et al.*, Nucl. Phys. A **632**, 229 (1998).
[47] G. D. Dracoulis, C. Fahlander, and M. P. Fewell, Nucl. Phys. A **383**, 119 (1982).
[48] D. G. Popescu *et al.*, Phys. Rev. C **55**, 1175 (1997).
[49] R. A. O'neil and D. G. Burke, Nucl. Phys. A **182**, 342 (1972).
[50] N. L. Gjørup, P. M. Walker, G. Sletten, M. A. Bentley, B. Fabricius, and J. F. Sharpey-Schafer, Nucl. Phys. A **582**, 369 (1995).
[51] G. D. Dracoulis *et al.*, Phys. Rev. C **81**, 054313 (2010).
[52] J. K. Deng *et al.*, Phys. Rev. C **52**, 595 (1995).
[53] K. Jain, O. Burglin, G. D. Dracoulis, B. Fabricius, N. Rowley, and P. M. Walker, Nucl. Phys. A **591**, 61 (1995).
[54] Ts. Venkova *et al.*, Z. Phys. A **344**, 417 (1993).
[55] F. R. Xu, E. G. Zhao, R. Wyss, and P. M. Walker, Phys. Rev. Lett. **92**, 252501 (2004).
[56] A. N. Andreyev *et al.*, Phys. Rev. Lett. **82**, 1819 (1999).
[57] N. Fotiades *et al.*, Phys. Rev. C **56**, 723 (1997).